Paper

Ground Fault Discrimination based on Wavelet Transform using Artificial Neural Networks

Student Member Ampol Tungkanawanich (Osaka University)
Member Zen-Ichiro Kawasaki (Osaka University)
Life Member Kenji Matsuura (Osaka University)
Non-member Hitoshi Kuno (Kansai Tech Corporation)

Wavelet transform is one of the most efficient tools for analyzing non-stationary signals such as transients, and has been widely applied to solve numerous problems in power systems. This paper demonstrates a novel application of wavelet transform to identify the causes of ground faults in power distribution systems. The discrimination scheme which can automatically recognize the fault causes is proposed using artificial neural networks. The scheme can be separated into two stages, the time-frequency analysis of transients by wavelet transform and the pattern recognition to identify the causes of faults. By using the actual fault data, it is shown that the proposed method provides satisfactory results for identifying the fault causes. Moreover, the results obtained by this method are useful to explain the mechanisms of faults simultaneously.

Keywords: ground faults, zero-sequence current, wavelet transform, dynamic spectrum, automatic discrimination scheme, artificial neural networks.

1. Introduction

Ground faults have been considered as ones of the main problems in power distribution systems and account for more than 80 [%] of all faults. They affect the reliability, security and quality of power systems.[1-3] Ground faults can be caused by various sources for examples, animal and tree contact, the failure of electrical equipment, etc. When a fault occurs, the faulted section or circuit can be generally identified.[4-6] In case that the fault is permanent, a dispatch of personnel to the suspected site is needed to recover the system. Therefore the prior knowledge of fault causes is essential to allow the appropriate recovering actions to be taken, saving unnecessary costs, such as power system down-time cost. In order to discriminate the causes of ground faults, the signal-processing technique to the detected fault signals has been applied. It was investigated that the characteristics of zero-sequence current and voltage are uniquely dependent on the cause of fault and therefore they can be used for the purpose of fault cause identification.[1] M. Watanabe et al. observed the waveforms of zero-sequence current and used their total harmonic distortion by Fourier transform to recognize the causes of faults.[1] Another method was proposed in [2] by comparing the phase plane trajectory of zero-sequence current waveforms.

Generally, meaningful information is contained in fault signals during transient periods that are naturally non-stationary signals due to the sudden changes of fault aspect and ground fault route. Therefore the transient should be considered while identifying fault causes. We discussed that the methods in [1,2] that randomly consider one cycle of fault signal may be inadequate. The more efficient discrimination method based on fault transients requires a suitable signal-processing technique to be developed and wavelet transform is one of the algorithms that possibly solve this problem. Wavelet transform is a useful tool for analyzing non-stationary signals in both time and frequency domains based on the basic function named *mother wavelet*. Recently, the use of wavelet transform has been widely applied to many problems in power systems such as power quality assessment[7], analysis of electromagnetic power system transients[8], power distribution relaying[9], fault location[10], etc.

In this paper, we present a new method based on wavelet transform for identifying the causes of ground faults. The continuous wavelet transform[11-15] is used to extract all specific harmonics of zero-sequence current transients, and provides the time-varying information of harmonics. It is demonstrated that the time-frequency analysis result or *dynamic spectrum* has its own unique characteristics and can be used to identify the causes of faults. The influence of weather condition on dynamic spectra and the equivalent circuits at the points of ground faults are additionally discussed. Moreover, we propose the automatic discrimination scheme by using artificial neural networks. By using the actual fault data collected in Kansai area, it is shown that the proposed scheme can provide satisfactory results for identifying the causes of faults, and clarify the mechanisms of faults simultaneously.

2. Fault Signal Acquisition System

In Japan, the non-grounded distribution system is

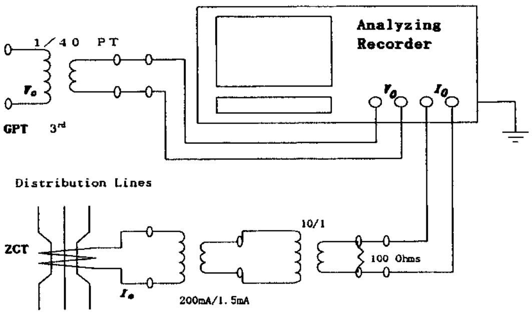

Fig. 1. A fault signal acquisition system.

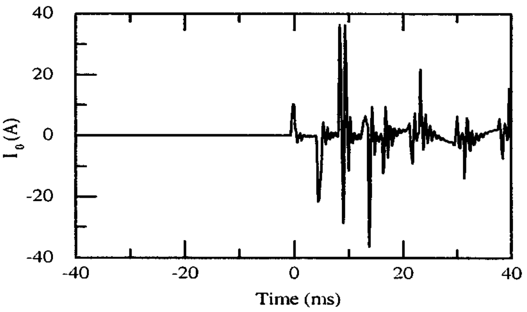

Fig. 2. An example of zero-sequence current waveform (inferior insulator and breaking of cable).

mostly adopted. Generally, the distributed substation receives the electric power at the high voltage around 20∼154 kV from the first or second step substation and usually sends it to the customers at the high voltage 6.6 kV. Each year in the service area of Kansai electric power company, which covers the main cities such as Osaka, Kyoto and Kobe, there are a great number of faults occurred. The remote observation system is installed to automatically detect a fault in the substation. Once a fault occurs, the zero-sequence current (I_0) and voltage (V_0) signals that are generally well known as the significant data in fault cause analysis will be recorded. Their definitions are expressed as

$$\mathbf{I}_0 = \frac{\mathbf{I}_u + \mathbf{I}_v + \mathbf{I}_w}{3} \quad , \quad \mathbf{V}_0 = \frac{\mathbf{V}_u + \mathbf{V}_v + \mathbf{V}_w}{3} \quad (1)$$

where, $\mathbf{I}_u$, $\mathbf{I}_v$, $\mathbf{I}_w$ and $\mathbf{V}_u$, $\mathbf{V}_v$, $\mathbf{V}_w$ are the current and voltage phasors of each phase, respectively.

Fig. 1 shows a fault signal acquisition system. Zero-sequence current transformer (ZCT) and grounded potential transformer (GPT) are used to simultaneously measure I_0 and V_0, respectively. The data is digitized at 5 kHz sampling rate and is recorded by an analyzing recorder (Yokogawa: AR1600) for 1.6 s. Fig. 2 shows an example of zero-sequence current waveforms obtained by this system.

3. Fault Cause Discrimination by Wavelet Transform

Conventionally, Fourier transform is applied for fault analysis.[1,9] In case of transients that are usually non-stationary signals, the study of time-varying information is required and it seems to be insufficient if only Fourier transform is utilized. The wavelet transform overcomes the limitation of Fourier transform by employing the analyzing functions, which localize in both time and frequency domains. These analyzing functions are generated in the form of translations and dilations of a basic function, the so-called *mother wavelet*. Thus wavelet transform is applied in many areas to analyze the non-stationary signals.[7-10] In this paper, we employ the continuous wavelet transform to extract the dynamic spectra of fault signals. The continuous wavelet transform of function x(t) with mother wavelet ψ(t) is expressed as

$$CWT(f,b) = \sqrt{2\pi f}\int_{-\infty}^{\infty} \psi^*[2\pi f(t-b)]x(t)dt \quad (2)$$

where f is frequency, b is time parameter, and (*) denotes a complex conjugate. The selected mother wavelet should be a fast-decaying oscillation function. In this study, we apply one of the family of complex Gabor functions as shown in (3) to be mother wavelet, because it is considered as an optimal window for time-localization and accordant with the function used in Fourier transform.[12]

$$\psi(t) = e^{-\frac{t^2}{64}}\, e^{\mathrm{it}} \quad \cdots\cdots\cdots\cdots \quad (3)$$

In this paper, we concentrate on the zero-sequence current waveforms, because it was investigated based on the actual data of ground fault waveforms that there are more remarkable changes in zero-sequence current than zero-sequence voltage according to fault causes.[1] Table 1 shows the fault data and their causes we used in this paper. The time-frequency analysis of zero-sequence current was performed. A result is called *a dynamic spectrum* because wavelet analysis derives a spectrum as a function of time. The computation of the first 40 ms of fault event with interval 0.2 ms and the frequency range 60-2400 Hz with interval 60 Hz was determined. Fig. 3 shows typical examples of dynamic spectra of zero sequence current resulting from different causes expressed by contour maps. The value on the contour map represents the relative intensity of power spectrum normalized by that in case of fundamental frequency (60Hz) at that time. As a result, we know both the quantity and timing of harmonics. Moreover, we can describe the mechanisms of ground faults as follows.

3.1 Inferior air switch An example of dynamic spectra of this fault cause is illustrated in Fig. 3 (a). The dynamic spectrum consists of harmonics (60-2000

Table 1. Fault data with their causes (30 data).

Fault cause	Number of data
1. Inferior air switch (inferior porcelain)	18
2. Inferior three-pole HV cutout (inferior porcelain)	4
3. Breaking of cable	4
4. Tree contacting	3
5. Inferior insulator and breaking of cable (two causes included)	1

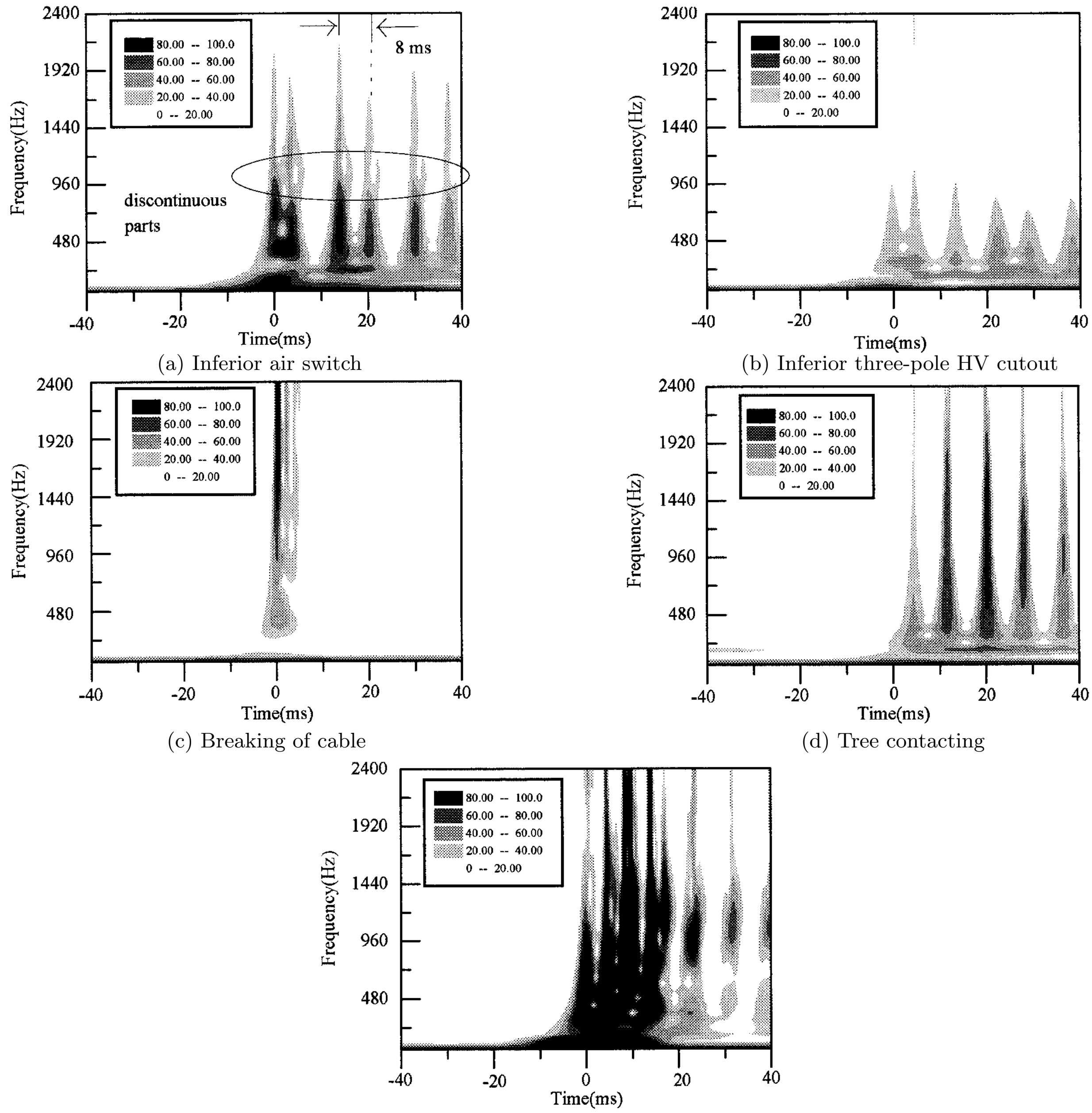

(a) Inferior air switch

(b) Inferior three-pole HV cutout

(c) Breaking of cable

(d) Tree contacting

(e) Inferior insulator and breaking of cable

Fig. 3. Examples of dynamic spectra of zero sequence current resulting from different causes.

Hz) with quantity more than 20 [%] appearing in a period of 8 ms.

3.2 Inferior three-pole HV cutout Fig. 3 (b) shows an example of dynamic spectra in this case. We obtain the similar result as Fig. 3 (a) but the range of harmonics is 60-1000 Hz.

From Fig. 3 (a) and (b), we discuss that the periods of these harmonics are systematically related to the 16 ms period of the distribution system (60 Hz system). We postulate that when the distribution voltage exceeds the threshold value, the current will flow through the point of ground fault, causing an event that resembles discharge phenomenon. For these two cases, the faults were caused by insulation degradation (inferior porcelain). It is discussed that the discharge occurred at the aperture of the defective parts, which include voids in porcelain and the stained surface. In addition, there are discontinuous parts on the contour map in a specific frequency region (720-1200 Hz) in Fig. 3 (a). We think that they depend on the shape of defective parts and the type of porcelain material. From this point of view, it is advantageous to know more clearly about the kind of faulty equipment.

3.3 Breaking of cable The dynamic spectrum in case of breaking of cable is shown in Fig. 3 (c). In this case, the harmonics do not change periodically and there is only one pulse at the beginning of the fault event. This fault phenomenon is definitely different from those of (a) and (b). We discuss that the ground fault happened through resistance and the pulse was caused by uncompleted contact in the first stage. After that, the fault point contacted to the ground. As a re-

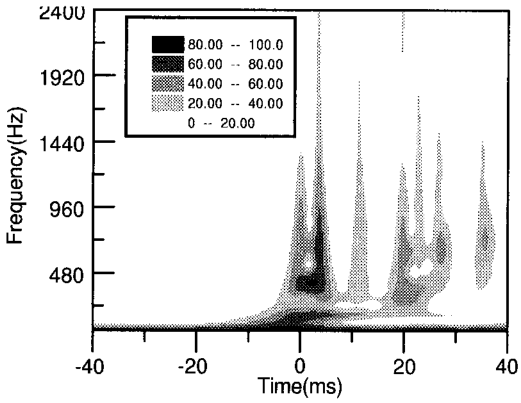

Fig. 4. The dynamic spectrum of zero-sequence current under no rain (inferior air switch).

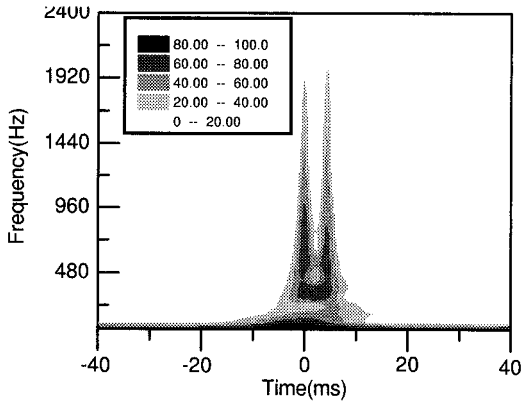

Fig. 5. The dynamic spectrum of zero-sequence current under rain (tree contacting).

sult, nothing appears in dynamic spectrum afterwards.

3.4 Tree contacting Fig. 3 (d) shows an example of dynamic spectra obtained from the fault caused by tree contacting. In this result, the 60-2400 Hz harmonics appears in a period of 8 ms. Although the result resembles those in (a) and (b), the variation of harmonics is smoother and the width of dynamic spectrum is narrower. We argue that the aperture of contact caused the discharge. It is discussed that the discharge occurred only at an aperture of a contact and the structure of a discharge gap was not complicated as those in (a) and (b).

3.5 Inferior insulator and breaking of cable Fig. 3 (e) shows the dynamic spectrum of this case. Although the 60-2400 Hz harmonics with high quantity occurs periodically, their periods have no relation with the system period in the first stage (0-20 ms). Because there were two simultaneous causes of ground faults, we think that the ground faults occurred at several points and the current flowed through ground more than one route in the beginning. After 20 ms, the periodic phenomenon, which is similar to those in (a) and (b), occurred. In this stage, we discuss that it was influenced by the inferior insulator only. It is obviously seen that the dynamic spectrum is different from all cases above.

In conclusion, the dynamic spectra of zero-sequence current have the special characteristics to identify the causes of faults and are useful to explain the fault mechanisms.

4. Interpretation and Discussion

4.1 Influence of weather condition on dynamic spectra The influence of weather condition such as precipitation on dynamic spectra is discussed. In all cases of faults except tree contacting, there is a tendency that the quantity of higher harmonics seems to be lower if there is no rain. For example, Fig. 4 shows a dynamic spectrum of zero-sequence current under no rain in case of inferior air switch. This result is different from the typical example in Fig. 3 (a) that the harmonics appear unsteadily with less quantity. Concerning the feature of this fault, it is caused by the insulation deterioration (inferior porcelain). If there is rain or the humidity increases, the surface resistance of porcelain becomes low. The leakage current flows through the surface of an insulator and then will be cut off due to the surface drying (because of the heat generated by this leakage current itself). This repeated phenomenon is known as *scintillation discharge*.[16] Therefore, without such a kind of this discharge, the dynamic spectrum in case of no rain exhibits lower quantity of harmonics.

On the contrary, in case of tree contacting, the reverse result is obtained. Most of them occurred under no rain. Fig. 5 shows the dynamic spectrum of zero-sequence current under rain. This result differs from the typical example in Fig. 3 (d) that the higher harmonics appear only in the first 10 ms of fault event. Considering the fault nature, this fault is caused by the discharge of air gap between electric cable and tree at the contacted point. When there is rain, the resistance through the air gap becomes low. The current then flows more easily and continuously, leading to the dissolution of discharge. From these results, the weather condition should be considered while analyzing fault causes based on dynamic spectra.

4.2 The equivalent circuits at the points of ground faults Fig. 6 illustrates the ideas and equivalent circuits at the points of ground faults of some cases. In case of inferior air switch and three pole HV cutout, the faults were caused by inferior porcelain. There are some voids (air gaps) in porcelain part and the capacitance components (C_a, C_b, C_c) indicate the voids which are connected in series and parallel as shown in Fig. 6 (a). The capacitance C_s is assumed as the discharge along stained surface caused by salt damage and rain. Concerning the fault caused by breaking of cable, the broken cable did not contact to ground perfectly at the first stage. Therefore its equivalent circuit is the fast switch operated at transient as shown in Fig. 6 (b). Fig. 6 (c) shows an equivalent circuit in case of tree contacting. The capacitance component (C) is assumed as the air gap between tree and electric cable. Finally, the parallel combination of (a) and (b) can be utilized as an equivalent circuit in case of inferior insulator and breaking of cable. Note that the damping time constant of fault current on each period

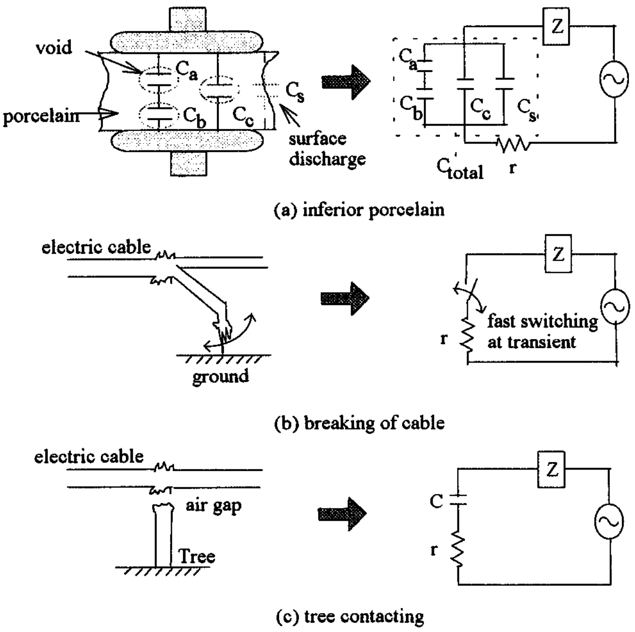

Fig. 6. The ideas and equivalent circuits at ground fault points of some cases.

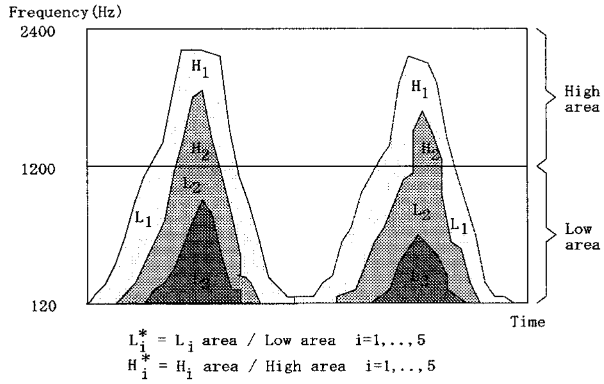

Fig. 7. Definition of neural network inputs.

Table 2. Labeling method.

The value on contour map (p)	Labeled symbol
$20 \leqq p < 40$	L_1
$40 \leqq p < 60$	L_2
$60 \leqq p < 80$	L_3
$80 \leqq p < 100$	L_4
$p \geqq 100$	L_5

increases if the multiplication result of capacitance and resistance increases. As shown in Fig. 3, the width of dynamic spectra in case of inferior porcelain as shown in Fig. 3 (a) and (b) is broader than that of tree contacting in Fig. 3 (d). It is discussed that the total capacitance obtained from parallel connection in case of inferior porcelain is larger than that in case of tree contacting.

5. Automatic Discrimination Scheme by Artificial Neural Networks

Normally, the fault nature is complicated and the knowledge about it is not easily transferable from person to person. Therefore, it is convenient and necessary to implement an automatic fault-discrimination system so that the faults can be correctly recognized even though there is no expert in the office. In this section, artificial neural networks[17,18] are applied to recognize the causes of faults based on pattern recognition of dynamic spectra. The artificial neural networks are suitable to identify the causes of faults because of their capability to learn and recognize the highly nonlinear and complicated models such as fault features. Moreover, they are flexible to be improved based on new information.

5.1 Selection of input data and training data sets To recognize the patterns by neural networks, the selection of input data sets is important. The appropriate inputs should be effective to represent the characteristic of pattern and meaningful to the cause of fault. Considering Fig. 3, the number of elements in dynamic spectrum is very large because of the computation on the time and frequency domains. Thus it is difficult to use all elements as the inputs of neural network. We propose to construct the input data sets by separating the frequency region in 2 levels, high and low, as shown in Fig. 7. The values of dynamic spectrum in the low frequency region are labeled as L_1,..,L_5 by the rule shown in Table 2. For the high frequency region, the symbols H_1,..,H_5 are used to label in the same way. The densities of labels in their own region (L^*_1,..,L^*_5,H^*_1,..,H^*_5) are used to be the inputs of network. To construct training data, the effective training data that can represent the main characteristics of fault causes are inevitable. Therefore, the average value of some of the most results is chosen. The numbers of the data used to construct the training data and the recognized data are indicated in Table 3. Fig. 8 shows the training data sets of all causes.

5.2 Design of neural network structure In this paper, the structure of three-layer networks as shown in Fig. 9 is used. The neural networks were designed to have 10 input, 10∼50 hidden, and 5 output neurons. Back propagation algorithm was applied to train the networks with learning rate $\eta = 0.2$ and momentum rate $\alpha = 0.9$.[17] The sigmoid function was used as a neuron transfer function. The back propagation is an iterative gradient algorithm designed to minimize a cost function (here is the mean square error between the actual output of network and the desired output). If a node corresponds to the expected cause, the desired output of that node is set to be 0.9, else it is set to be 0.1. The least mean square error was set at 0.1 to conditionally stop the training procedure.

5.3 Results and discussions Table 4 indicates the recognition results by various networks and the most correct results are acquired by the networks with 10, 30 and 40 hidden neurons. It shows that the better result may not be obtained though the hidden neurons increase. The high accuracy 80 [%] can be achieved. However, it is difficult to conclude that this scheme is reliable because of the very few data in some causes. To solve this problem, the test of further data by simula-

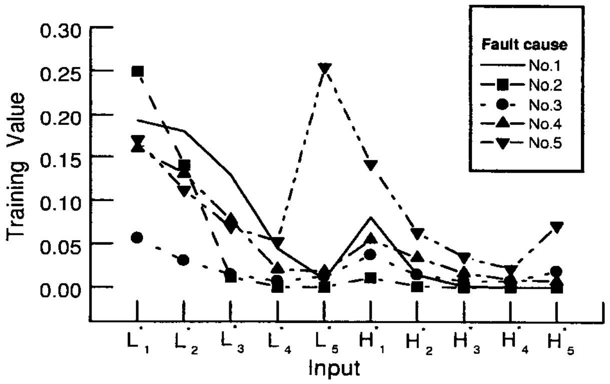

Fig. 8. Training data of each fault cause.

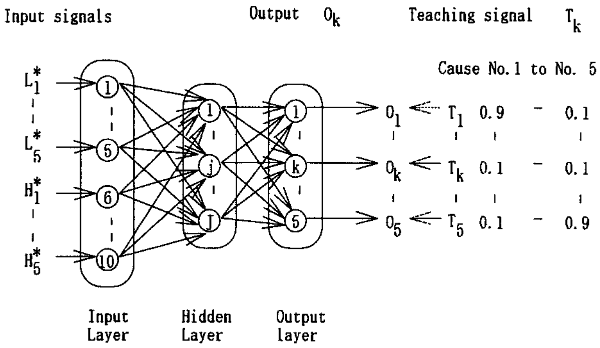

Fig. 9. The structure of proposed neural network.

tion is purposed to generalize the scheme and will be explained in next subsection.

5.4 Test of further data by simulation The efficiency of neural networks means the ability to recognize patterns which were not encountered during the training period. Neural networks often require the large number of examples to be able to have a reasonably fair concept of its reliability. Therefore, the simulation scheme that is similar to the method in [18] is adopted to conquer this problem. With each input data as a template, additional patterns were generated by superimposing random noise ± 10 [%] to all ten inputs, and the new patterns continue to belong to the original cause. The network with 10 hidden neurons was utilized to recognize these new patterns, and the results are shown in Table 5. The scheme shows satisfactory results that provide high accuracy to correctly recognize 228 patterns from 300 patterns or 76 [%]. The accuracy is little lower than that in case of no noises. Moreover, it is useful to know how much error deviating from the actual data that we can still correctly recognize. We therefore determined the recognition results while adding the random noises ± 5 [%] and ± 20 [%] to the data. The new patterns were recognized by the same method. The accurate rates, 79.0 [%] and 75.7 [%], are obtained in case of noises ± 5 [%] and ± 20 [%], respectively. The scheme is shown to be reliable to some degree because it can almost recognize the causes of faults correctly under noise interference.

Table 3. Number of data used to construct training data and recognized data (30 data).

Fault cause	Data used to construct training data	Recognized data	Total
No.1	8	10	18
No.2	2	2	4
No.3	2	2	4
No.4	2	1	3
No.5	1	0	1

Table 4. The recognition results by various networks.

Fault cause	Number of data	Number of correctly recognized data				
		HN10	HN20	HN30	HN40	HN50
No.1	18	15	14	15	15	14
No.2	4	3	3	3	3	3
No.3	4	3	3	3	3	3
No.4	3	2	2	2	2	2
No.5	1	1	1	1	1	1
Total	30	**24**	23	**24**	**24**	23

Note: HN = the number of hidden neurons.

Table 5. The recognition results of new patterns generated by adding ± 10 [%] noises.

Fault cause	Template of new random patterns					
	Data used to construct training patterns		Recognized data		Total	
	In	Correct	In	Correct	In	Correct
No.1	80	79	100	64	180	143
No.2	20	20	20	5	40	25
No.3	20	20	20	10	40	30
No.4	20	20	10	0	30	20
No.5	10	10	0	0	10	10
Total	150	149	150	79	**300**	**228**

5.5 Comparison the results with conventional method The conventional method, which is Fourier transform, was applied to discriminate the fault causes. We utilized ten data sets, including the spectral intensities of odd-ordered harmonics from 3 to 19 and total harmonic distortion of them as the inputs of neural networks. By using the similar model of neural networks, we obtain the accuracy 76.7 [%] which is little lower than that by wavelet transform (80 [%]). Based on available data, the recognition result by wavelet transform seems to be not different from that obtained by Fourier transform. However, the accuracy is hopeful to be improved because we can additionally get the time-varying information of harmonics from wavelet analysis. The more appropriate inputs of neural networks can be investigated from this additional information when the new fault data are collected.

6. Conclusions

Novel scheme for discriminating the causes of ground faults has been introduced. The proposed scheme is based on the time-frequency analysis results or dynamic spectra of zero-sequence current obtained by wavelet transform. We conclude the main concepts of this paper as follows.

6.1 Dynamic spectrum provides the time-varying information of each harmonic, which is difficult to be obtained by conventional Fourier transform, and can be used as a new method for discriminating fault causes. Besides, the dynamic spectrum is advantageous to explain the fault mechanism and the kind of faulty part. The weather condition also influences the dynamic spectra so it should be considered while analyzing fault causes.

6.2 The equivalent circuits at the points of ground faults have been proposed based on dynamic spectra and they are useful to understand the physical meanings of faults.

6.3 In order to construct the automatic discrimination scheme, the three-layer neural networks were utilized to recognize the patterns of dynamic spectra. It has been shown that the proposed system is effective to discriminate fault causes with the accuracy 80 [%] in case of inferior air switch, inferior three-pole HV cutout, inferior electric cable, tree contacting, inferior insulator with breaking of cable. Based on available data, although the discrimination accuracy by the proposed method is only little higher than that by Fourier transform, this method is hopeful to increase the accuracy.

6.4 To generalize and improve the proposed scheme, more fault signal acquisition systems are required to be installed to accumulate the fault data. The more appropriate inputs of neural networks, that can effectively represent the characteristic of the dynamic spectrum, should be examined based on the new information of fault signals.

7. Acknowledgments

The authors would like to acknowledge the Kansai electric power company for valuable data. The authors would also like to express their hearty thanks to Dr. Masatake Kawada (Nagoya Institute of Technology) and the reviewers of this paper for their instructive comments and suggestions.

(Manuscript received August 17, 1999, revised June 21, 2000)

References

(1) M. Watanabe, K. Kotanshi, O. Nakamura, H. Kurioka, S. Hukui, K. Tsuji, *A new method for discrimination of ground faults causes in distribution line*, Trans. IEE Japan, Vol.115-B, No.1, 1995, pp. 18-23 (in Japanese).

(2) T. Horita, M. Sumiyoshi, T. Wakai, N. Ikeda, I. Kitamura, *A new classification method of ground faults in distribution lines with phase plane trajectory of their waveforms*, Trans. IEE Japan, Vol.117-B, No.2, 1997, pp. 196-202 (in Japanese).

(3) Mo-yuen Chow, Sue O. Yee, Leroy S. Taylor, *Recognizing animal-caused faults in power distribution systems using artificial neural networks*, IEEE Trans. on Power Delivery, Vol. 8, No. 3, July 1993, pp. 1268-1273.

(4) Adly A. Girgis, Melisa B. Johns, *A hybrid expert system for faulted section identification, fault type classification and selection of fault location algorithms*, IEEE Trans. on Power Delivery, Vol. 4, No. 2, April 1989, pp. 978-985.

(5) Yuan-Yih Hsu, F.C. Lu, Y. Chien, J.P. Liu, J.T. Lin, H.S. Yu, R.T. Kuo, *An expert system for locating distribution system faults*, IEEE Trans. on Power Delivery, Vol. 6, No. 1, January 1991, pp. 366-372.

(6) Hong-Tzer Yang, Wen-Yeau Chang, Chiang-Lien Huang, *A new neural networks approach to on-line fault section estimation using information of protective relays and circuit breakers*, IEEE Trans. on Power Delivery, Vol. 9, No. 1, January 1994, pp. 220-229.

(7) S. Santoso, Edward J. Powers, W. Mack Grady, Peter Hofmann, *Power quality assessment via wavelet transform analysis*, IEEE Trans. on Power Delivery, Vol.11, No.2, April 1996, pp. 924-930.

(8) David C. Robertson, Octavia I. Camps, Jeffrey S. Mayer, William B. Gish, *Wavelets and electromagnetic power system transients*, IEEE Trans. on Power Delivery, Vol. 11, No.2, April 1996, pp. 1050-1058.

(9) Oinis Chaari, Michel Meunier, Francoise Brouaye, *Wavelet : A new tool for the resonant grounded power distribution systems relaying*, IEEE Trans. on Power Delivery, Vol.11, No.3, July 1996, pp. 1301-1308.

(10) Fernando H. Magnago, Ali Abur, *Fault location using wavelets*, IEEE Trans. on Power Delivery, Vol. 13, No. 4, October 1998, pp. 1475-1480.

(11) C. Sidney Burrus, *Introduction to wavelets and wavelet transforms, a primer*, Prentice Hall, Inc. , 1998.

(12) Charles K. Chui, *An introduction to wavelets*, Academic Press, Inc. , 1992.

(13) A. Tungkanawanich, M. Kawada, Z-I Kawasaki, K. Matsuura, H. Kuno, K. Oku, *A new diagnosis method of ground fault causes on distribution line using wavelet transform*, Proceedings of the international conference of electrical engineering 1998(ICEE'98), No. P-B 9, pp. 293-296.

(14) A. Tungkanawanich, Z-I. Kawasaki, K. Matsuura, H. Kuno, *Experimental study for transient phenomena of ground faults on distribution lines based on various fault causes*, Proceedings of the IEEE Budapest power tech'99 conference, Session 22, No. BPT99-311-33, p. 146.

(15) A. Tungkanawanich, Z-I. Kawasaki, K. Matsuura, M. Kawada, H. Kuno, K. Oku, *Discrimination of ground fault cause on distribution line by wavelet transform*, Trans. IEE Japan, Vol.118-B, No.9, 1998, pp. 1060-1061 (Technical letter in Japanese).

(16) M. Kosaki, *Inter university: High voltage and insulation engineering*, Ohm Press, 1997(in Japanese).

(17) Richard P. Lippman, *An introduction to computing with neural nets*, IEEE ASSP Magazine, April 1987, pp. 4-22.

(18) L. Satish, Walter S. Zaengl, *Artificial neural networks for recognition of 3-d partial discharge patterns*, IEEE Trans. on Dielectrics and Electrical Insulation, Vol.1, No.2, April 1994, pp. 265-275.

Ampol Tungkanawanich (Student Member) received a bachelor degree in Electrical Engineering (B.E.) from Chulalongkorn University (Thailand) in 1995 and a master degree in Electrical Engineering, Osaka University in 1999 where he is presently a Ph.D. student. His research mainly deals with fault analysis on power systems, partial discharge and signal processing.

Zen-Ichiro Kawasaki (Member) received his B.S., M.S. and Dr. Eng. degrees in Electrical Engineering from Osaka University in 1973, 1975 and 1978, respectively. In 1989, he joined the Department of Electrical Engineering, Osaka University and is currently an associate professor. His research mainly concerns the observation of lightning, and the diagnosis techniques for power equipment. Dr. Kawasaki is also a member of the Society of Atmospheric Electricity of Japan.

Kenji Matsuura (Life Member) received his B.S. and M.S. degrees in Electrical Engineering from Osaka University in 1960 and 1962, respectively. In 1977, he joined the Department of Electrical Engineering, Osaka University and is currently a professor. His research concerns the generation, transmission, and control of electric power. Dr. Matsuura is a member of the Institute of Energy and Resources.

Hitoshi Kuno (Non-member) received B.S. in Electrical Engineering from Nihonbunri University and joined Kansai Tech Corporation in 1990. Mr. Kuno is currently a member of the technical development research group. His research is mainly in fault diagnosis on distribution line.